Available online at www.sciencedirect.com

ScienceDirect

Procedia Engineering 157 (2016) 114 – 121

Procedia Engineering

www.elsevier.com/locate/procedia

IX International Conference on Computational Heat and Mass Transfer, ICCHMT2016

The enthalpy-porosity method applied to the modelling of the ice slurry melting process during tube flow

Beata Niezgoda-Żelasko *

Institute of Thermal and Process Engineering, Krakow University of Technology, al. Jana Pawła II 37, , Poland, Kraków 31-864

Abstract

The ice slurry heat transfer process in flow can be described as forced convection heat transfer of a non-Newtonian fluid subject to phase change (melting of ice crystals). This paper looks at the application of the enthalpy-porosity method to the modelling of the melting process occurring during homogenous tube flow of ice slurry. It will discuss experimentally verified results of thermal calculations, including the distribution of temperature values, heat transfer coefficients and changes to the content of solid particles. The results of the calculations apply to the laminar and turbulent flow areas, various initial mass fractions of ice and various tube cross-section shapes.

Peer-review under responsibility of the organizing committee of ICCHMT2016

Keywords: Heat transfer; Melting, Modeling, The enthalpy-porosity method;

1. Introduction

Slurry ice is classified as a heat carrier (coolant). As a heat transfer medium, it demonstrates the heat properties characteristic of refrigerants, including high thermal capacity, as well as high values of thermal conductivity and heat transfer coefficients. Ice slurry is a mixture of water ice crystals and water, or water with an addition of a freezing point reducer (salt, glycol or alcohol). Ice slurry is a non-Newtonian fluid. It is treated as a rheologically stable fluid. The Bingham model is the rheological model most frequently applied to ice slurry. Studies of heat transfer during the melting of flowing ice slurry include experimental work performed to determine the heat transfer coefficients and how they are influenced by parameters such as the mass fraction of ice, flow velocity and heat flux density.

* Corresponding author. Tel.: +48 12 628 3588; fax: +48 12 628 2071.
E-mail address: bniezgo@mech.pk.edu.pl

Peer-review under responsibility of the organizing committee of ICCHMT2016
doi:10.1016/j.proeng.2016.08.346

Nomenclature

a	thermal diffusivity (m^2/s)
a,b	height and width of the slit channel (m)
A_{mush}	mushy ice surface area constant (Pa s/m^2)
h_{ref}	reference enthalpy (J/kg)
k_H	consistency index in the Herschel-Buckley model ($Ns^{n'}/m^2$)
L, L_T	tube length, thermal measurement length (m)
n'	flow index, (-)
Re_B	Reynolds number for ice slurry, $Re_B = uD_h\rho_B / \mu_B$
r	heat of ice melting (J/kg), coordinate in a cylindrical coordinate system (m)
$\dot{q}_m$	average heat flux density (W/m^2)
T_s	temperature at which melting starts (K)
T_L	temperature at the end of the melting process (K)
$\bar{v}_p$	solid phase removal velocity vector
x	geometrical coordinate (m)
x_a	carrying fluid concentration (%)
x_s	mass fraction of ice (%)
α	heat transfer coefficient ($W/(m^2 \cdot K)$)
α_s	volume fraction of solid phase in mixture (%), $\alpha_s = \left(1+\left(1-x_s\right)\rho_s /(x_s\rho_a)\right)^{-1}$
β	porosity index (-)
ε	is a small number in equations (6-7) (ε=0.001) to prevent division by zero
μ_p	plastic viscosity (Pa·s)
$k_{B,u}$	heat conductivity of ice slurry at flow velocity $u\neq 0$ ($W/(m \cdot K)$)
$k_{B,u=0}$	heat conductivity of ice slurry at flow velocity $u=0$ ($W/(m \cdot K)$)
$Pe_{B,u}$	Peclet number of movable ice slurry, $Pe_{B,u} = \dot{\gamma} D_s^{\,2} / a_a$
Subscripts	
a	carrying fluid
B	Bingham fluid, ice slurry
eff	effective
i	internal
m	mixture; mean value

The available body of literature includes few studies focusing on flow and thermal process modelling for ice slurry. In paper [1] Ismail and Radwan proposes an analytical solution to motion and energy equations in the process of formation of ice crystals in a laminar ice slurry film. Kitanovski and Poredos [2] presents a mathematical model of the segregation of solid particles in heterogeneous ice slurry flow. Niezgoda-Żelasko and Zalewski [3] and Wnag et al. [4] discuss CFD modelling of adiabatic ice slurry flow relying on a single-phase model [3] and multi-phase models, i.e. a mixture [4] and an Euler-Euler model [3]. Only Niezgoda-Żelasko with Żelasko [5] and Zhang with Shi [6] discuss the results of the modelling of the ice slurry melting process under forced convection conditions in tubes. Niezgoda-Żelasko with Żelasko [5] presents the results of the modelling of a single-phase melting process of Bingham fluid ice slurry. Zhang with Shi [6] concerns the modelling of heat transfer in ice slurry using a multi-phase Euler-Euler model. The calculation results shown in [6] were validated with the results of the experiments described in [5] and [7]. The use of the multi-phase model is especially justified in the case of the heterogeneous flow of ice slurry. The formation of heterogeneous flow is promoted by large pipe diameters, low flow velocity, low mass fractions of ice and large solid particle sizes. Figure 1 shows the limit curves $u_m(\alpha_s)_{Di}$ of heterogeneous and homogenous flow in a pipe with a diameter of D_i=0.016 m for ice slurry containing solid particles of $0{,}1<D_s<0{,}15$ mm [2],[8]. In practical applications (e.g. in supply installations and heat exchangers), homogenous ice slurry flow is recommended in the laminar flow zone [8]. In said flow zone, the enthalpy-porosity method may be an alternative for the Euler-Euler model used in the modelling of the melting of ice slurry.

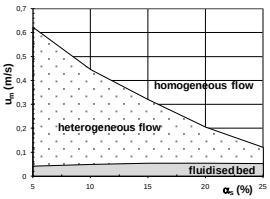

Fig. 1. Limit curves $u_m(\alpha_s)$ of heterogeneous and homogenous flow D_i=0.016 m, 0.1<D_s<0.15 mm.

The ice slurry heat transfer process in flow can be described as forced convection heat transfer of a non-Newtonian fluid subject to phase change (melting of ice crystals). In the modelling of the ice slurry heat transfer process, it is necessary to take into account the change in the physical properties of the fluid, including the content of solid particles, as well as the specific rheological properties and the micro-convection of ice particles in the moving liquid, causing an increase in the ice slurry heat transfer coefficient values. The paper expands on the author's research described in [5], focusing on experimental verification and on the application of UDF procedures to the modelling of the ice slurry melting process.

2. Ice slurry flow and heat transfer

The original results of the thermal studies presented here apply to an ice slurry made of a 10.6% aqueous solution of ethanol with a mass fractions of ice of $0 \le x_s \le 30\%$, with an average ice crystal size (width-length) of D_s=0.1 - 0.15 mm. A detailed description and analysis of the results of the experimental studies for flow through pipes and rectangular channels has been presented in [3], [5] and [9]. The experimental program included measurements of flow and thermal parameters for ice slurry flowing, among other things, through:

- copper pipes with the diameter of D_i = 0.016 m and the length of L=4.6 m (thermal measurement length L_T=2.32 m), $\dot{q}_m$ =5000W/m^2.
- a tube with a rectangular (slit) cross-section, with the following dimensions: axb=0.003x0.0358m, L= 2.0 m (L_T=0.65 m), $\dot{q}_m$ =4760W/m^2

a

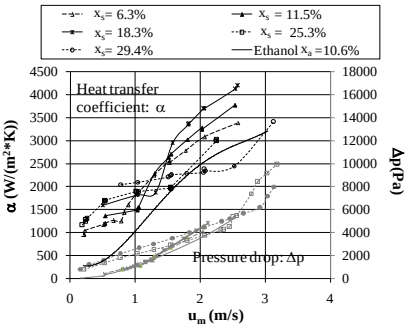

b

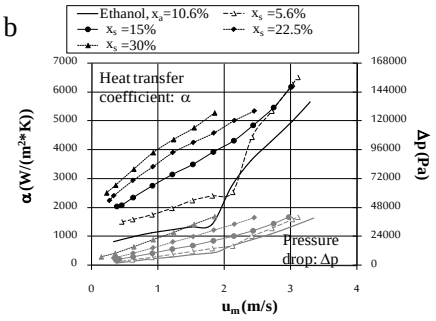

Fig. 2. (a) Pressure drop and heat transfer coefficients as a function of u_m and x_s; D_i=0,016 m;
(b) Pressure drop and heat transfer coefficients as a function of u_m and x_s; slit channel.

The heat stream was supplied to the external surface of the channels using a heating cable. For the slit channel, only its top part was heated. The thermal studies included the determination of heat transfer coefficients in the final stretch of the thermal measurement length, after a fully developed velocity and temperature profile was obtained. At the inlet and outlet of the measurement length, the temperature of the core of the ice slurry stream was measured along with the temperature of the heat transfer surface and the mass fraction of ice [3], [5], [9]. For the slit channel, the temperature of the heated channel wall was additionally measured along its axis of symmetry at 0.295, 0.455 and 0.62 m from the start point of the thermal measurement length. The heat transfer coefficient was calculated using the equation:

$$\alpha_{x=L} = \dot{q}_{\mathrm{m}} / \left(T_{\mathrm{w}} - T_{\mathrm{f}}\right) \tag{1}$$

Figures 2a and 2b present pressure drops and heat transfer coefficients as a function of the flow velocity of the solid mass fraction for pipe and slit channel flow, respectively.
The results allowed for the following description of the heat transfer process for the ice slurry:
- the change in α depending on the varying ice fraction x_{s} is clearer in the laminar region,
- in the turbulent region, the values of heat transfer coefficients correlate more strongly with flow velocity than with the mass fraction of solid particles,
- except for the intermediate flow region, the $\alpha(x_{\mathrm{s}})$ function is an increasing one,
- in the case of ice content x_{s} > 10-20%, at the same flow velocity, the heat transfer coefficients of the slurry can be lower than those of the carrying fluid. This is observed when the ice slurry and the carrying fluid flows have a different character [8], [9].

3. Modeling of heat transfer

The ice slurry melting process in straight tube flow was modelled using Fluent software with the "enthalpy-porosity" formulation [10-13]. In this method, the liquid fraction is computed based on energy balance. In addition, an intermediate region (the mushy zone), in which the liquid fraction lies between 0 and 1, is introduced. The mushy zone is treated as a "pseudo" porous medium, with porosity equal to the liquid fraction, changing from 0 to 1 as the material melts.

For the considered problem, the energy equation has the following form:

$$\frac{\partial}{\partial t} \cdot \left(\rho \cdot h\right) + \nabla \cdot \left(\rho \cdot \vec{u} \cdot h\right) = \nabla\left(k \cdot \nabla T\right) - S_E \tag{2}$$

$$S_E = \frac{\partial\left(\rho \beta r\right)}{\partial t} + \nabla\left(\rho \vec{u} \beta r\right). \tag{3}$$

The mass enthalpy of the material is computed from the equation:

$$h = h_{\mathrm{ref}} + \int_{T_{\mathrm{ref}}}^{T} c_{\mathrm{p}} \cdot dT + \beta \cdot r\,. \tag{4}$$

and the liquid fraction can be defined as:

$$\beta = \begin{cases} \dfrac{T - T_{\mathrm{s}}}{T_{\mathrm{L}} - T_{\mathrm{s}}} & T_{\mathrm{s}} < T < T_{\mathrm{L}} \\ 0 & T < T_s\,. \\ 1 & T_{\mathrm{L}} < T \end{cases} \tag{5}$$

In the case of forced convection, equation (2) must be closed with a momentum equation, to which an appropriate term is added to account for the pressure drop caused by the presence of solid material. The relationship between the porosity and momentum change in the mushy zone takes on the following form:

$$S = \frac{\left(1-\beta\right)^2}{\left(\beta^3 + \varepsilon\right)} * A_{\mathrm{mush}} * \left(\vec{u} - \vec{u}_{\mathrm{p}}\right) \tag{6}$$

The terms added to the turbulence equations in the mushy and solidified zones are similar to equation (6) and can be written as:

$$S = \frac{(1-\beta)^2}{(\beta^3+\varepsilon)} * A_{\text{mush}} * \Phi \tag{7}$$

The above method can be used to solve melting/solidification problems of mixtures with variable melting temperatures, treated as homogeneous materials with substituted physical properties (ρ, c_p, k, μ). In order to improve the agreement between the calculations and experiments for ice slurry of initial concentration x_{ai} = 10.6%, density and specific heat were made temperature-dependent [5], [8]. Equations for density and specific heat are an approximiation of the tabular data of ethanol-based ice slurry and an aqueous solution of ethanol published in [14], [15], [16], [17], [18], [19].

It should be noted that the presence of solid particles in a moving mixture causes an increase in the heat conductivity coefficient, which can be several times greater than the value resulting from the Maxwell-Tareff equation [20]. For moving mixtures, the heat conductivity coefficient is defined by equation (8) [21]:

$$\frac{k_{B,u}}{k_{B,u=0}} = \begin{cases} 1+3\left(\alpha/100\right)\text{Pe}_{B,u}^{\ 1.5} & \text{Pe}_{B,u} < 0.67 \\ 1+1.8\left(\alpha/100\right)\text{Pe}_{B,u}^{\ 0.18} & 0.67 \le \text{Pe}_{B,u} \le 250 \\ 1+3\left(\alpha/100\right)\text{Pe}_{B,u}^{\ 1/11} & 250 \le \text{Pe}_{B,u} \end{cases} \tag{8}$$

The physical properties taken into consideration in melting process modeling also include temperature T_s (at which the melting starts) and T_L (end of the melting process), in accordance with eq.(5). In this case, it was assumed that for ethanol solution x_{ai} =10.6%, T_L=268.39 K, while T_s - was each time determined in such a way that the liquid fraction calculated from (5) corresponded to the parameters $1-\beta = x_s/100$ and $T_{in}=T$ at the inlet to the measuring length.

In agreement with the principles of adiabatic flow modeling, it was assumed that:

- In the case of laminar flow, the fluid is treated as a Herschell-Buckley liquid with consistency index $k_H = \mu_p$ [8], [9], flow index n' = 1 and yield shear stress τ_p [8], [9]. The values μ_p, τ_p were only made dependent on the mean experimental value of ice content x_s [3].
- In the case of turbulent flow and the RNG k-ε turbulence model, the dynamic viscosity of the suspension was computed from the Vande equation (15) [2].

Heat transfer in the ice slurry was modeled using Fluent software with the above sets of equations and our own UDF procedures, which take account of the impact of T, x_s, $\dot{\gamma}$ on the physical properties of the ice slurry.

Due to the geometry of the pipe and the slit channel (a/b=0.084), the heat transfer process was modelled in 2D. The assumed boundary conditions at the inlet and outlet of the measuring length and corresponding to the experimental data for the pipe and the slit channel have been shown in figure 3.

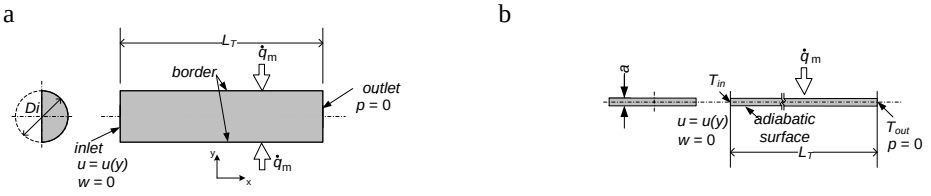

Fig. 3. The boundary conditions assumed for the calculations: (a) pipe D_i = 0.016 m; (b) slit channel axb=0.003x0.0358 m

Velocity at the inlet to the thermal measurement length corresponded to a fully developed velocity profile obtained by adiabatic flow modeling. The obtained temperature distribution in the fluid and on the wall enables the value of the heat transfer coefficient at a chosen measuring point to be computed from equation (1). The calculations were performed for all the channel shapes taken into consideration and the temperature values obtained from the measurements.

4. Calculation results

Figure 4a shows a comparison of computed (using the Fluent software) and experimental heat transfer coefficients. Sample temperature distributions in tube cross-section x =2.3 m, at u_m = 0.5 m/s for different mass fractions x_s of ice, are shown in Figure 4b.

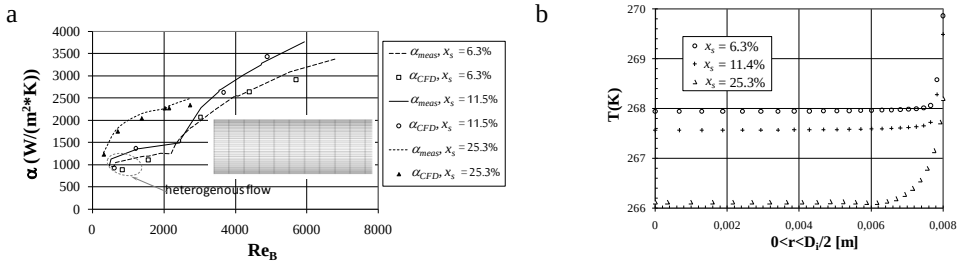

Fig. 4. (a) Calculated and measured values of heat transfer coefficients, tube D_i = 0.016 m;
(b) Cross-sectional temperature distribution x = 2.3 m at u_m = 1.5 m/s and various ice fractions.

The effect of the melting process and of a specific velocity profile on conductivity is shown in Figure 5. A non-monotonic function $k_{B,u}(r)$ follows from equation (8), according to which the values of heat conductivity for slurries are proportional to the shear rate (i.e. for flow inside circular pipes to the value of the expression $\partial u/\partial r$). It should be noted that the highest absolute shear rate values occur at the boundary layer. For r=0 the shear rate equals zero (the maximum velocity value). If the melting process does not occur, the highest heat conductivity values are recorded at the pipe wall, while the lowest occur at its axis of symmetry (Figure 5a).

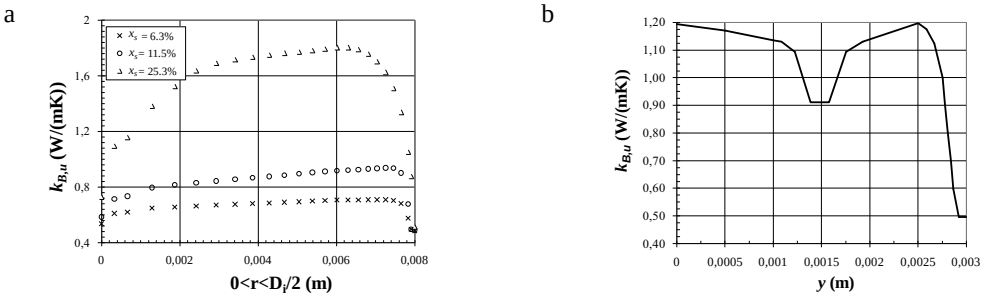

Fig. 5. Cross-sectional distribution of heat conductivity of ice slurry: (a) pipe flow, x = 2.3 m for various ice fractions and mean velocity u_m = 1.5 m/s; (b) rectangular flow cross-section x = 0,62 m, u_m = 1.5 m/s, x_s=15%

When ice is melted at the boundary layer, the ethanol solution flows in the vicinity of the wall, while the ice slurry flows inside the core. At the boundary of the unmelted ice, the heat conductivity value reaches its maximum: $k_{B,u}(x_s$=6.3% = 0.7 W/(mK); $k_{B,u}(x_s$=25.3%)=1.81 W/(mK). The lowest value of coefficient k corresponds to the value of heat conductivity for ethanol whose temperature equals that of the wall (e.g. k_a=0.47-0.49 W/(mK)). Precisely at the pipe axis, the value of the medium's heat conductivity corresponds to the value of $k_{B,u=0}$ ($k_{B,u=0}(x_s$=6.3%)=0.54 W/(mK); $k_{B,u=0}(x_s$=25.3%)= 0.72 W/(mK)). At the boundary of the unmelted ice, the heat conductivity value reaches its maximum: $k_{B,u}(x_s$=6.3% = 0.7 W/(mK); $k_{B,u}(x_s$=25.3%)=1.81 W/(mK). The lowest value of coefficient k corresponds to the value of heat conductivity for ethanol whose temperature equals that of the wall (e.g. k_a=0.47-0.49 W/(mK)). Precisely at the pipe axis, the value of the medium's heat conductivity corresponds to the value of $k_{B,u=0}$ ($k_{B,u=0}(x_s$=6.3%)=0.54 W/(mK); $k_{B,u=0}(x_s$=25.3%)= 0.72 W/(mK)).

Results of the simulation of adiabatic flow of ice slurry through a rectangular channel axb=0.003x0.0358 m indicate that the velocity of the ice slurry $u(x)$ is constant for more than 80% of points along the length of the channel with a rectangular cross-section [9]. Hence, the ice slurry heat transfer process for the a/b=0.084 cross-section was modelled in 2D. Analyses of a slit channel made it possible to verify the distribution of temperature on its non-adiabatic wall. Sample verification of the temperature profile $T_w(x)$ (on the vertical plane of symmetry) for a

30% ice slurry and a mean velocity of u_m=0.45; 0.93; 1.54 m/s has been shown in Figure 6a. The experimentally measured temperatures of the heat transfer surface indicate that the temperature profile develops faster under actual conditions, as compared to the computed values. This may be due to the adoption of a flat geometrical model for the calculations. Under real-life conditions, the flow of the ice slurry is more turbulent, which corresponds to shorter hydraulic and thermal stabilization lengths, as well as more intensive cooling of the heat transfer surface area.
Figure 6b present the mass share of the liquid phase in the mixture along the length of the slit channel for a mass fraction of ice of x_s=15%. For a 15% ice slurry, in the final 35% of the measurement length, the ice fully melted at the channel wall .

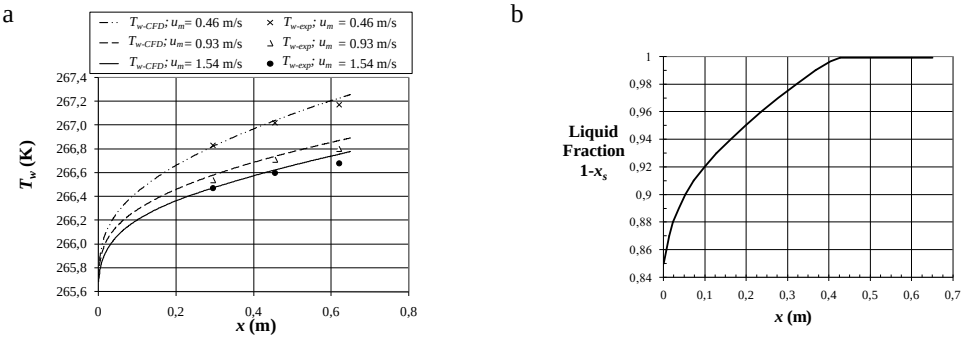

Fig. 6.(a) Experimental verification of the computed temperature profiles $T_w(x)$ for a 30% ice slurry;
(b) Change in the share of the liquid phase (1-x_s) at the heated wall of the channel u_m = 1.5 m/s, x_s=15%.

The change in the heat conductivity coefficient of the ice slurry in the rectangular channel, shown in Figure 5b, results from equation (8), the velocity profile of the ice slurry in the slit channel and the adopted geometrical model of the channel. Due to the asymmetry of the thermal boundary conditions, the geometrical model of the channel used in the heat transfer modelling process corresponded to its full height *a*. Hence, the values of the $k_{B,u}(y)$ function on the one hand result from the extreme shear rate at the channel walls and on the other hand from the impact of the solid particle content and temperature on the heat conductivity coefficients of the immobile slurry.

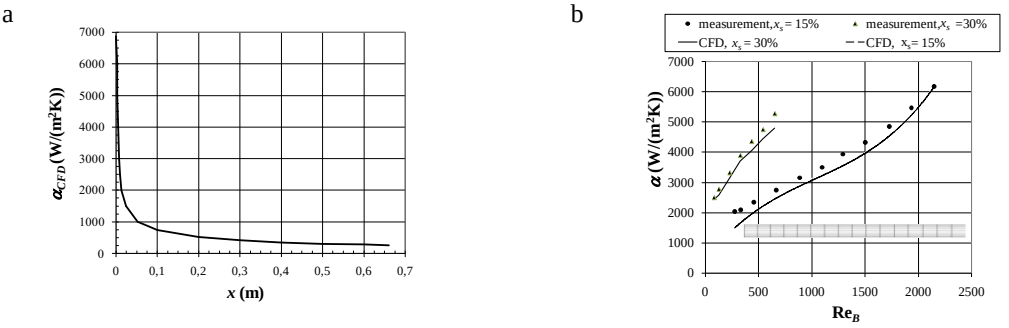

Fig. 7. Heat transfer coefficient: (a) Change α(x) on a vertical plane of symmetry x=0,62m, u_m = 1.5 m/s, x_s=15%; (b) Measured and computed heat transfer coefficients of the ice slurry: slit channel - *a*x*b*=0.003x0.0358 m, *x*=0.62 m

Figure 7a present local values of heat transfer coefficients and the mass share of the liquid phase in the mixture along the length of the slit channel for a mass fraction of ice of x_s=15%. Figure 7b compares the measured and computed heat transfer coefficients for a 15% and 30% ice slurry in a slit channel. The values of the computed heat transfer coefficients shown in Figure 7 are lower than the measured heat transfer coefficients. This relationship between the measured and computed heat transfer coefficients is a consequence of the correlation between the experimentally determined and computed temperature profiles of the heated channel wall $T_w(x)$ (cf. fig. 6a). The relative difference between the measured and computed heat transfer coefficients will not exceed 8.9% in this case.

5. Conclusions

The CFD simulations of heat transfer in ice slurry flow in horizontal tubes were performed using a single-phase flow model and the enthalpy-porosity technique. In the case of laminar flow, the Bingham model was selected and calculations were conducted using our own, experimentally derived values of μ_p and τ_p. In the turbulent region, the viscosity was evaluated on the basis of the Vande relationship, and the assumed turbulence model was the RNG k-ε model with enhanced wall treatment. The aim of the modeling was to determine the heat transfer coefficients on the basis of the temperature field distribution in the fluid. The calculation results were verified through qualitative assessment of the changes in heat conductivity coefficients in a rectangular flow cross-section, the consistency of temperature distribution on the heat transfer surface for the slit channel and the consistency of the measured and calculated heat transfer coefficients. The discrepancy between computational and experimental results for heat transfer coefficients in both the laminar and turbulent region, did not exceed 10%.

Acknowledgments

The research was carried out as part of research project PB 0759/T10/2002/23 funded by the State Committee for Scientific Research Polish National Science Centre.

References

1. K.A.R Ismail, M.M Radwan, Effect of axial conduction on the ice crystal growth in laminar falling films, Int. J. of Refrigeration, 22 (1999) 389-401.
2. A. Kitanovski, A. Poredos, Concentration distribution and viscosity of ice-slurry in heterogeneous flow. Int. J. of Refrigeration, 25 (2002) 827-35.
3. B. Niezgoda-Żelasko, W. Zalewski, Momentum transfer of ice slurry flows in tubes - modelling. Int. J. of Refrigeration, 29 (2006) 429-436.
4. J. Wang, T. Zhang, S. Wang, Heterogeneous ice slurry flow and concentration distribution in horizontal pipes, Int. J. of Heat and Fluid Flow, 44 (2013) 425-434.
5. B. Niezgoda-Żelasko, Heat transfer of ice slurry flows in tubes. Int. J. of Refrigeration, 29 (2006) 437-450.
6. P. Zhang, X.J. Shi , Thermo-fluidic characteristuc of ice slurry in horizontal circular pipes, Int. J. of Heat and Mass Transfer, 89 (2015) 950-963.
7. E. Stamatiou, M. Kawaji, Thermal and flow behavior of ice slurries in a vertical rectangular channel. Part I: Local distribution measurements in adiabatic flow, Int. J. Heat Mass Tran., 48 (2005) 3527-3543.
8. B. Niezgoda-Żelasko, Wymiana ciepła i opory przepływu zawiesiny lodowej w przewodach, Monografia 334, Politechnika Krakowska, Kraków, 2006.
9. B. Niezgoda-Żelasko, J. Żelasko, Melting of ice slurry under forced convection conditions in tubes, Exp. Thermal And Fluid Science, 32 (2008) 1597-1608.
10. Fluent Guide-Multiphase Flow Regimes, 2003.
11. C. R. Swaminathan, V. R. Voller, A General Enthalpy Method for Modeling Solidification Processes. Metallurgical Transactions B, 23B (1992) 651-664.
12. V. Voller, C. Prakash, A Fixed-Grid Numerical Modeling Methodology for Convection-Diffusion Mushy Region Phase-Change Problems. Int. J. Heat Mass Transfer, 30 (1987) 1709-1720.
13. V. R .Voller, C. R. Swaminathan, Generalized Source-Based Method for Solidification Phase Change. Numer. Heat Transfer B, 19 (1991) 175-189.
14. O. Bel, A. Lallemand, Etude d'un fluide frigoporteur disphasique. 1:Caracteristiques thermophysiques inttrinseques d'un coulis de glace, International Journal of Refrigeration, 22 (1999) 164-174.
15. A. Melinder, E. Granryd, Using property values of aqueous solution and ice to estimate ice concentrations and enthalpies of ice slurries, International Journal of Refrigeration, 28 (2005) 13-19.
16. A. Melinder, Thermophysical properties of liquid secondary refrigerants, charts and tables, Swedish Society of Refrigeration, Stockholm, 1997.
17. R. Lugo, L. Fournaison, J.M. Chourot, , J. Guilpart, An excess function method to model the thermophysical properties of one-phase secondary refrigerants, International Journal of Refrigeration 25 (2002) 916-923.
18. VDI-Wärmeatlas, Düsseldorf, 1991
19. B. Niezgoda-Żelasko, M.Litwin, Właściwości termofizyczne lodu zawiesinowego na przykładzie mieszaniny woda-alkohol etylowy, Technika chłodnicza i klimatyzacyjna, 5 (2004) 162-168.
20. A.H. Skelland, Non-Newtonian Flow and Heat Transfer, John Wiley & Sons, Inc., New York, 1967
21 P.Charunyakorn, S. Sengupta, S.K. Roy, Forced convection heat transfer in microencapsulated phase change material slurries: flow in circular duct, Int. J. Heat Mass Transfer, 34 (1991) 819-833.